

Journal of İstanbul Faculty of Medicine İstanbul Tıp Fakültesi Dergisi

Research Article

Open Access

INVESTIGATING THE ANTICANCER EFFECTS OF 3-BROMOPYRUVIC ACID ON METABOLIC ALTERATIONS IN PANCREATIC CANCER CELLS *IN VITRO*

PANKREAS KANSERİ HÜCRELERİNDE 3-BROMOPÜRUVİK ASİDİN METABOLİK DEĞİŞİKLİKLER ÜZERİNDEKİ ANTİKANSER ETKİLERİNİN *İN VİTRO* OLARAK ARAŞTIRILMASI



Duygu Aydemir^{1,2,3} , Nuriye Nuray Uluşu^{2,3} 

¹ İstanbul University, Institute of Child Health, Department of Pediatric Basic Sciences, Division of Medical Genetics, İstanbul, Türkiye

² Koç University, School of Medicine, Department of Medical Biochemistry, İstanbul, Türkiye

³ Koç University Research Center for Translational Medicine (KUTTAM), İstanbul, Türkiye

Abstract

Objective: Pancreatic ductal adenocarcinoma (PDAC) is one of the most aggressive cancers, characterised by a high mortality rate and resistance to chemotherapeutics. Frequent mutations in *TP53*, *SMAD4*, and *CDKN2A* drive metabolic reprogramming and contribute to tumour progression and treatment resistance. Hexokinase 2 (HK2), a key glycolytic enzyme, is commonly overexpressed in PDAC and represents a promising therapeutic target. This study aimed to investigate the anticancer effects of 3-bromopyruvic acid (3-BrPA) on metabolic pathways, oxidative stress, and ferroptosis in BXP-3 PDAC cells harbouring *TP53*, *SMAD4*, and *CDKN2A* mutations.

Material and Methods: BXP-3 cells were administered with various concentrations of 3-BrPA, and cell viability was assessed using the MTT assay to determine the IC_{50} . The morphological changes were evaluated via light microscopy. HK2 expression and the enzymatic activities of GST, G6PD, 6-PGD, and GR were measured, along with the glutathione redox status and intracellular iron levels. CPT1C activity was additionally assessed to evaluate the metabolic alterations associated with the fatty acid oxidation pathways.

Results: 3-BrPA administration significantly decreased cell viability in a dose-dependent manner and downregulated HK2 expression. It inhibited glycolysis and the pentose phosphate pathway enzymes, reduced the antioxidant capacity, and elevated oxidative stress markers. These changes were associated with increased intracellular iron levels and decreased GSH/GSSG ratios, indicat-

Öz

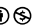
Amaç: Pankreatik duktal adenokarsinom (PDAC), yüksek mortalite oranı ve kemoterapötiklere karşı direnç ile karakterize edilen en agresif kanser türlerinden biridir. *TP53*, *SMAD4* ve *CDKN2A* genlerindeki sık mutasyonlar, metabolik yeniden programlamayı tetikleyerek tümör progresyonuna ve tedaviye karşı direnç gelişimine katkıda bulunur. Glikolizin kilit enzimlerinden biri olan Heksokinaz 2 (HK2), PDAC'da sıklıkla aşırı eksprese edilir ve umut verici bir terapötik hedef olarak öne çıkar. Bu çalışma, *TP53*, *SMAD4* ve *CDKN2A* mutasyonlarını taşıyan BXP-3 PDAC hücrelerinde 3-bromopürivik asidin (3-BrPA) metabolik yollar, oksidatif stres ve ferroptosis üzerindeki antikanser etkilerini araştırmayı amaçlamıştır.

Gereç ve Yöntemler: BXP-3 hücreleri farklı konsantrasyonlarda 3-BrPA ile muamele edilmiştir. Hücre canlılığı, IC_{50} değerinin belirlenmesi amacıyla MTT testi ile değerlendirilmiştir. Morfolojik değişiklikler ışık mikroskobu ile incelenmiştir. HK2 ekspresyonu ile birlikte GST, G6PD, 6-PGD ve GR enzimlerinin aktiviteleri ölçülmüş; glutatyon redoks durumu ve hücre içi demir seviyeleri değerlendirilmiştir. Ayrıca, yağ asidi oksidasyonu yoluyla metabolik kompensasyonu değerlendirmek üzere CPT1C aktivitesi analiz edilmiştir.

Bulgular: 3-BrPA uygulaması, doz bağımlı şekilde hücre canlılığını anlamlı düzeyde azaltmış ve HK2 ekspresyonunu baskılamıştır. Glikoliz ve pentoz fosfat yolunun enzimatik aktiviteleri inhibe edilmiş; antioksidan kapasite azalmış ve oksidatif stres belirteçleri artmıştır. Bu değişiklikler, hücre içi demir düzeylerinde artış



“ Citation: Aydemir D, Uluşu NN. Investigating the anticancer effects of 3-bromopyruvic acid on metabolic alterations in pancreatic cancer cells *in vitro*. Journal of İstanbul Faculty of Medicine 2025;88(3):207-215. <https://doi.org/10.26650/IUITFD.1703970>

© This work is licensed under Creative Commons Attribution-NonCommercial 4.0 International License. 

© 2025. Aydemir D, Uluşu NN.

✉ Corresponding author: Duygu Aydemir duygu.aydemir@istanbul.edu.tr



ing the induction of ferroptosis. Furthermore, CPT1C activity was upregulated, indicating increased fatty acid oxidation.

Conclusion: Our findings demonstrate that 3-BrPA disrupts glucose metabolism, induces oxidative stress, and triggers ferroptosis in PDAC cells through HK2 inhibition. This study highlights 3-BrPA's therapeutic potential in targeting cancer metabolism and ferroptosis.

Keywords Pancreatic ductal adenocarcinoma • 3-bromopyruvic acid • hexokinase 2 inhibitors • ferroptosis • oxidative stress • pentose phosphate pathway

INTRODUCTION

Pancreatic cancer is one of the most lethal and aggressive malignancies with an extremely poor prognosis and an alarmingly high mortality rate, approaching nearly 100%. The 5-year survival rate remains below 5%, underscoring the limited efficacy of current therapeutic interventions. Pancreatic ductal adenocarcinoma (PDAC) constitutes approximately 90% of all pancreatic cancer cases and, because of its increasing incidence and therapeutic resistance, is projected to become the second most prevalent cancer type globally within the next decade (1). Surgical resection followed by adjuvant chemotherapy is currently regarded as the most effective therapeutic strategy for pancreatic ductal adenocarcinoma (PDAC). However, due to the disease's typically late presentation, characterised by nonspecific symptoms and an overall poor prognosis, only approximately 10%–15% of patients are eligible for surgical intervention. For patients who are not candidates for surgery, gemcitabine (2',2'-difluoro-2'-deoxycytidine; GEM) is considered the standard first-line chemotherapeutic agent. Nevertheless, GEM therapy is associated with limited clinical benefit, primarily due to the rapid development of drug resistance, which is often attributed to reduced cellular uptake and a notably short plasma half-life of approximately 17 min (2).

Approximately 80% of pancreatic cancer patients develop chemoresistance during the locally advanced or metastatic stages of the disease, resulting in a median survival time of six months or less. Because this alarming statistic underscores the urgent need for more effective therapeutic strategies, the development of novel treatment approaches targeting PDAC has emerged as one of the most pressing challenges in contemporary oncology. A growing body of research is dedicated to overcoming chemoresistance and improving clinical outcomes, with a particular focus on extending the survival and quality of life of patients diagnosed with PDAC (3). Mothers against decapentaplegic homologue 4 (SMAD4),

ve GSH/GSSG oranında azalma ile birlikte gözlenmiş; ferroptozis indüksiyonunu işaret etmiştir. Ayrıca, CPT1C aktivitesinde artış saptanmıştır, bu da yağ asidi oksidasyonuna yönelik bir metabolik kaymaya işaret etmektedir.

Sonuç: Elde edilen bulgular, 3-BrPA'nın HK2 inhibisyonu yoluyla glukoz metabolizmasını bozduğunu, oksidatif stresi artırarak ferroptozisi tetiklediğini ortaya koymaktadır. Bu çalışma, 3-BrPA'nın kanser metabolizması ve ferroptozisi hedefleyen terapötik potansiyeline dikkat çekmektedir.

Anahtar Kelimeler Pankreatik duktal adenokarsinom • 3-bromopirüvik asit • heksokinaz 2 inhibitörleri • ferroptozis • oksidatif stres • pentoz fosfat yolu

cyclin-dependent kinase inhibitor 2A (CDKN2A), and tumour suppressor protein 53 (TP53) genes are the most commonly mutated in PDAC (4).

P53 is the key tumour suppressor protein mutated in more than 50-75% of PDAC cases, regulating apoptosis, ferroptosis, cell cycle arrest, cellular senescence, and metabolic programming (5). Metabolic reprogramming/adaptation is one of the cancer hallmarks and occurs via the dysregulation of p53, SMAD4, and CDKN2A protein functions in the PDAC (6). P53 mutations are associated with elevated levels of HK2 and activation of HIF-1 α . Additionally, altered p53 function leads to elevated pentose phosphate pathway (PPP) metabolism because p53 can directly bind to the glucose 6-phosphate dehydrogenase (G6PD) to inhibit its activity and PPP (5). On the other hand, mutations in p53, SMAD4, and CDKN2A proteins lead to dysregulated glucose intake and enhance glycolytic enzymes via PI3K/Akt, HIF-1 α , GLUT1, HK1, HK2, phosphofructokinase, and LDH (7, 8). Furthermore, p53 has been shown to regulate the expression of carnitine palmitoyltransferase 1C (CPT1C), a member of the carnitine palmitoyltransferase (CPT) family that plays a crucial role in fatty acid oxidation (FAO). Reduced levels of CPT1C have been associated with increased cellular senescence, impaired mitochondrial function, and heightened cell death in cancer cells. While decreased activity of CPT1A is known to elevate oxidative stress, promote ferroptosis, and diminish antioxidant defences, there are currently no published data elucidating the role of CPT1C in these metabolic pathways specifically within pancreatic cancer cells (9).

Ferroptosis is increasingly recognised as a key driver of both chemoresistance and metastatic progression in PDAC. It is tightly controlled by oxidative stress, iron homeostasis, and lipid metabolism, and ferroptotic signaling is frequently impaired due to mutations in tumour suppressor genes such as TP53 and CDKN2A in PDAC. Given the iron-enriched microenvironment of the pancreatic tissue, therapeutic strategies targeting ferroptosis have gained considerable

interest. Ferroptosis is typically triggered by reduced antioxidant capacity, heightened oxidative stress, and the accumulation of iron and lipid peroxides. However, metabolic pathways such as glycolysis and PPP can inhibit ferroptosis by reinforcing cellular antioxidant defences, thereby promoting therapy resistance. Consequently, metabolic reprogramming to enhance ferroptotic sensitivity offers a promising strategy to overcome drug resistance in PDAC (10). Although increased ferroptosis has been correlated with the prognosis of PDAC, the exact role of ferroptosis and its molecular mechanisms has not been elucidated in pancreatic cancer (11).

Hexokinases (HKs) are evolutionarily conserved enzymes catalysing glycolysis's obligatory and rate-limiting step, where glucose is phosphorylated to glucose-6-phosphate (G6P). Both PPP and glycolysis use G6P. HK2 enzyme is highly expressed in PDAC cancers via upregulation of the PI3K/Akt pathway and can directly inhibit mitochondrial (intrinsic) apoptosis. HK2 upregulation is tightly associated with poor prognosis, chemoresistance, and metastasis in cancers; thus, targeting HK2 has gained attention as a promising therapeutic approach. Four main categories of HK2 inhibitors have been reported: glucose analogs, such as 2-deoxy-d-glucose (2-DG), non-coding regulated microRNAs, and 3-bromopyruvate (3-BrPA) and metformin. 3-BrPA, an alkylating agent, showed vigorous anti-tumour activity in several animal models, including pancreatic cancer (12). In this study, we aimed to investigate, for the first time in the literature, the effects of 3-BrPA on the BXP-3 harbouring mutations in TP53, SMAD4, and CDKN2A. This investigation sought to elucidate the potential of 3-BrPA as a therapeutic agent by examining its impact on key metabolic and cell death pathways in a genetically relevant PDAC model. Since G6P produced by HK2 is commonly used for the PPP and glycolysis pathways, inhibiting HK2 activity can block the three pathways and their intermediates, contributing to cancer progression and chemoresistance. Because ferroptosis contributes to metastasis and poor survival in PDAC, HK2 inhibitors may induce ferroptosis due to decreased PPP and glycolysis, which are responsible for the enhanced antioxidant status (13).

MATERIAL AND METHODS

Expanding and sub-culturing of the cells

BXP-3 cells were purchased from the American Type Culture Collection (ATCC). The indicated cells were cultured in RPMI medium supplemented with 5% heat-inactivated foetal bovine serum (FBS) and 1% penicillin-streptomycin. Cells were maintained at 37°C in a humidified incubator containing 5% CO₂. Sub-culturing was performed every 2–3

days upon reaching 80%–90% confluence to preserve cells in the logarithmic growth phase.

Evaluation of the cell viability

Cells were seeded (20,000 cells/per well) on the 96-well plates and, after 24 h, were treated with the increased concentration of 3-BrPA (0–300 µM) prepared in ultrapure water. BXP-3 cells were incubated with the indicated drugs for up to 48 h, and after incubation, 5 mg/mL 3-(4,5-Dimethylthiazol-2-yl)-2,5-Diphenyltetrazolium Bromide (MTT) solution was dissolved in PBS. The cell media was removed, and 50 µL of MTT solution and 150 µL of complete cell media were added onto the plates and incubated for 4 h. After incubation, DMSO-ethanol (1:1 v/v) solution (200 µL) was added to dissolve formazan, and its absorbance intensity at 600 nm was quantified. IC₅₀ values were calculated using GraphPad Prism (9.0) (n=4) (14).

Cell imaging

After calculating the IC₅₀ via the MTT assay, cells were seeded in the 25 cm² flasks and treated with selected concentrations of 3-BrPA below the IC₅₀ value, as 0, 1, 5, 10, 20, and 30 µM, for up to 48 h. Morphological assessments were conducted every 24 h using a light microscope to monitor cellular structure and viability. Representative images were captured daily to document changes in cell morphology and to support the qualitative evaluation of cellular health over time.

Measurement of the soluble protein concentration

The protein concentration in the cell lysates was quantified using the Pierce BCA Protein Assay Kit (Thermo Scientific, USA). Bovine serum albumin (BSA) was used as the standard for calibration, and the assay was performed following the manufacturer's instructions. Cell lysates were dispensed into 96-well microplates, and a Synergy H1 microplate reader (BioTek Instruments) was used to measure the absorbance at 562 nm.

Preparation of the cell lysates

BXP-3 cells were seeded in 25 cm² plates, and after 24 h, increased concentrations of 3-BrPA were administered to the cells for 48 h. The cell media was removed at the end of the incubation time, and an ice-cold PBS solution containing a protease inhibitor cocktail was added to the cells, which were then placed on ice. The cells were scraped off from the flask and transferred into clean Eppendorf tubes, then the cells were centrifuged at 2000 rpm for 10 min at +4°C. After centrifugation, the cell pellet was homogenised in sodium phosphate buffer (Na₂HPO₄/NaH₂PO₄, pH 7.4) supplemented with a protease inhibitor cocktail. The homogenate was subjected to sonication at 40% amplitude for 3 s to ensure

cell lysis and then centrifuged at $100,000 \times g$ for 1 h at $+4^{\circ}\text{C}$. Samples were stored at -80°C until the experiments were carried out.

Spectrophotometric measurement of the glucose 6-phosphate dehydrogenase activity

0.2 mM NADP⁺, 100 mM Tris-HCl buffer (pH 8.0), 0.6 mM G6P, and 10 mM MgCl₂ were used to evaluate the G6PD activity in the samples. Assays were duplicated, and NADPH production was followed at 340 nm at 37°C for 60 s. A Synergy H1 BIOTEK spectrophotometer measured the enzyme activity.

Determination of the 6-phosphogluconate dehydrogenase activity

A reaction mixture containing 0.2 mM NADP⁺, 0.6 mM 6PG, 10 mM MgCl₂, and 100 mM Tris-HCl buffer (pH 8.0) was prepared to evaluate the G6PD activity in the samples. The reaction was followed via NADPH production at 340 nm at 37°C for 60 s. A Synergy H1 BIOTEK spectrophotometer measured the enzyme activity. Assays were performed as duplicates, and specific enzyme activity was given as units/mg of protein.

Measurement of the glutathione-dependent antioxidant enzymes

The glutathione S-transferase (GST) activity was determined by the conjugation of reduced glutathione (GSH) with 1-chloro-2,4-dinitrobenzene (CDNB). A reaction mixture was prepared with 25 μl of 20 mM GSH, 0.2 M sodium phosphate buffer (pH 6.5), 25 μl of 20 mM CDNB, and cell lysate to measure the GST activity (15). 100 mM sodium phosphate buffer (pH 7.4), 1 mM oxidised glutathione (GSSG), and 0.2 mM NADPH were incubated with the cell lysates to measure the glutathione reductase (GR) activity (16). Assays were performed as duplicates, and specific enzyme activity was given as units/mg of protein.

ELISA

HK2 and CPT1C levels in the cell lysates treated with the HK2 inhibitor were measured via the ELISA technique, following the kit instructions.

Iron assay kit

Elevated iron levels are an indicator of both oxidative stress and ferroptosis. The iron content of the cytosol and mitochondria of the drug-treated cells will be measured following the kit instructions.

Statistical evaluation of the experimental data

Data were analysed using GraphPad Prism software (version 9.0), and statistical comparisons were performed using one-way analysis of variance (ANOVA), followed by Tukey's post hoc test for multiple comparisons. Results are presented as the mean \pm standard deviation (SD) from three independent replicates. A p-value of ≤ 0.05 was considered indicative of statistical significance. Each treatment group was compared to the control (CTL) and to each other. A p-value ≤ 0.05 was considered significant for each data point.

RESULTS

IC₅₀ value of the 3-BrPA on the pancreatic cancer cells

BXPC-3 cells were administered with various concentrations of 3-BrPA (0-300 μM) for up to 48 h. GraphPad Prism (version 9.0) was used to determine the cell viability, and the half-maximal inhibitory concentration (IC₅₀) of 3-BrPA was determined to be 40 μM (Figure 1). Based on this IC₅₀ value, subsequent experiments were conducted using 3-BrPA at concentrations of 1, 5, 10, 20, and 30 μM .

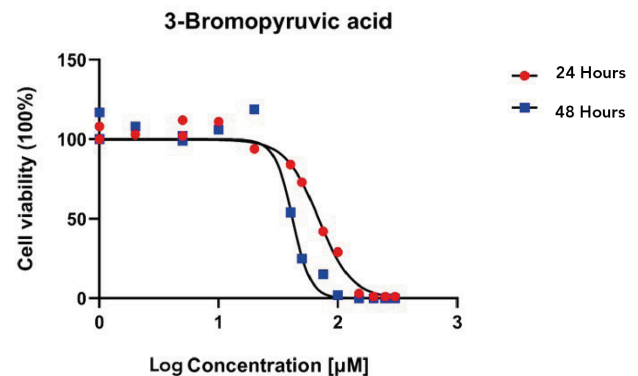


Figure 1. Concentration-dependent effects of 3-bromopyruvic acid (3-BrPA) on cell viability at 24 and 48 h. Cells were exposed to increasing concentrations of 3-BrPA (μM), and viability was assessed after 24 and 48 h using MTT. Data are presented as mean \pm standard deviation (SD) from 4 independent experiments. A progressive reduction in cell viability was observed in a concentration- and time-dependent manner, with greater cytotoxicity evident at the 48-h time point. The IC₅₀ value of 3-BrPA after 48 h was calculated as 40 μM .

Morphological changes indicating cell death in 3-BrPA-treated PDAC cells

BXPC-3 cells were exposed to escalating concentrations of 3-BrPA, and morphological changes indicative of cell death were observed using light microscopy. The MTT assay revealed that 3-BrPA induced a significant, dose-dependent decrease in cell viability compared with the untreated control group. Notably, concentrations of 20 and 30 μM elicited a marked cytotoxic

effect, highlighting the potent anti-proliferative activity of 3-BrPA in pancreatic ductal adenocarcinoma (PDAC) cells (Figure 2, Figure 3).

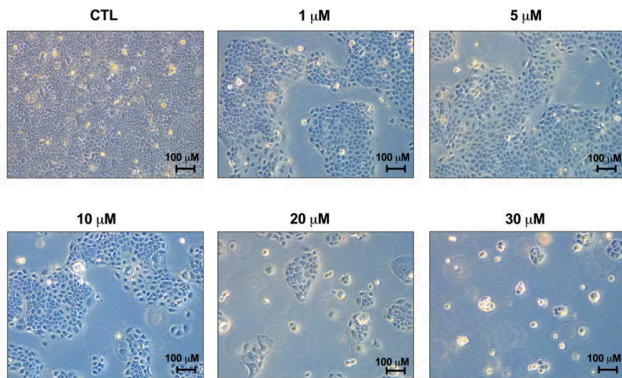


Figure 2. Representative images of control (CTL) and 3-bromopyruvic acid (3-BrPA)-treated cells. Cells were exposed to 0 (control), 1, 5, 10, 20, and 30 μM 3-BrPA for 48 h, and morphological changes were assessed using a light microscope. Compared with the untreated control, cells treated with increasing concentrations of 3-BrPA exhibited a progressive loss of confluence, with marked morphological deterioration at higher concentrations. Scale bar = 100 μm .

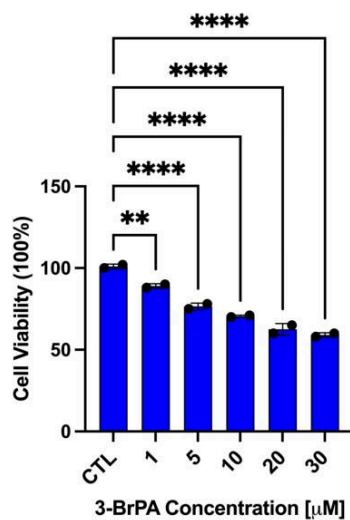


Figure 3. The effect of 3-bromopyruvic acid (3-BrPA) on cell viability was assessed following a 48-h exposure to increasing concentrations of 3-BrPA (μM). Cell viability (%) was determined using the MTT assay. Data are expressed as mean \pm standard deviation (SD) from four independent experiments. Treatment with 3-BrPA significantly decreased cell viability at all tested concentrations compared with the untreated control group, consistent with the morphological changes observed under light microscopy.

: $p < 0.001$, *: $p < 0.0001$

3-BrPA significantly decreased HK2 levels in the pancreatic cancer cells

HK2 expression levels were significantly reduced in cells treated with 3-BrPA, with the most pronounced decrease observed in the 20 μM and 30 μM treatment groups compared

with the control (Figure 4). 3-BrPA inhibited the enzyme activities responsible for PPP and glycolysis. G6PD and 6-PGD enzymes were analysed in HK2 inhibitor-treated cells to evaluate the glycolysis and PPP pathways. The indicated enzymes were significantly decreased in the 5, 20, and 30 μM dose groups compared with the control (Figure 5).

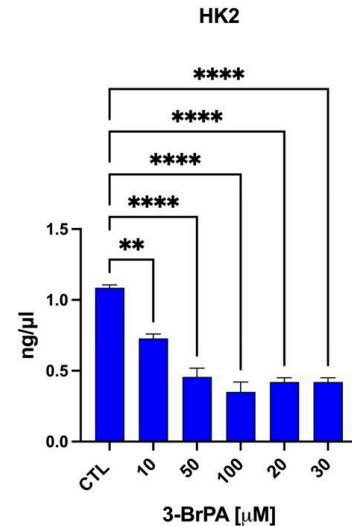


Figure 4. Hexokinase 2 (HK2) protein levels following treatment with varying concentrations of 3-bromopyruvic acid (3-BrPA). HK2 levels were quantified and expressed as ng/ μL after exposure to increasing concentrations of 3-BrPA (μM). Data represent mean \pm standard deviation (SD) from 4 independent experiments. A concentration-dependent change in the HK2 level expression was observed following 3-BrPA treatment.

*: $p \leq 0.05$, **: $p < 0.01$, ***: $p < 0.001$, ****: $p < 0.0001$

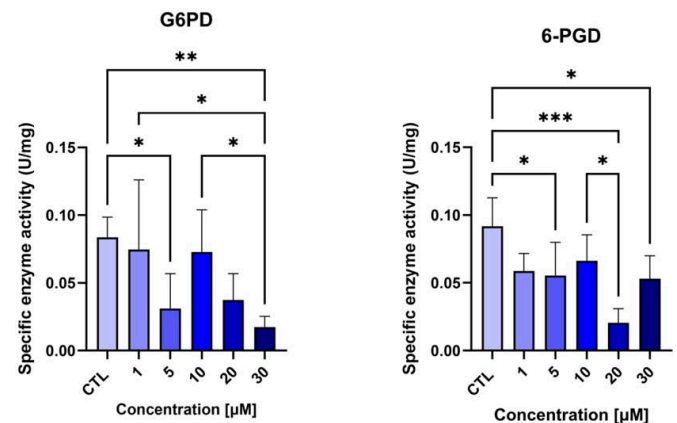


Figure 5. Specific activities of glucose-6-phosphate dehydrogenase (G6PD) and 6-phosphogluconate dehydrogenase (6-PGD) were evaluated following treatment with increasing concentrations of 3-bromopyruvic acid (3-BrPA). Enzyme activities were quantified and expressed as U/mg. Data are reported as mean \pm standard deviation (SD) from four independent experiments. Both G6PD and 6-PGD exhibited concentration-dependent alterations in enzymatic activity in response to 3-BrPA exposure.

* $p \leq 0.05$, ** $p < 0.01$, *** $p < 0.001$, **** $p < 0.0001$

HK2 inhibitor diminished the enzymatic activity involved in PPP and glycolysis

6-PGD and G6PD activities were measured to evaluate PPP and glycolysis pathways responding to HK2 inhibitor administration. 3-BrPA treatment reduced G6PD and 6-PGD activity in all dose groups. However, this decrease was significant in the 5, 20, and 30 μM dose groups compared with the control (Figure 5).

3-BrPA administration increased the oxidative stress and ferroptosis status of the PDAC cells

GR, GST, GSH/GSSG ratio, and Fe levels were measured to assess the oxidative stress levels and ferroptosis status of the PDAC cells upon HK2 inhibitor administration. GR activity decreased in all 3-BrPA-treated groups compared with the control, which was significant in the 20 and 30 μM dose groups (Figure 6). The GSH/GSSG ratio significantly decreased in all treated cells compared with the control group, except the one μM dose group (Figure 7). On the other hand, Fe levels significantly increased in all 3-BrPA-treated groups except 1 μM compared with the control (Figure 8).

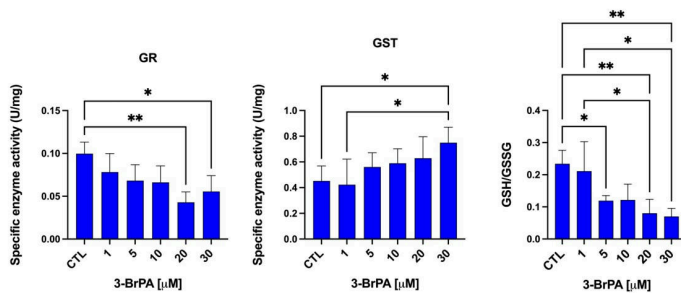


Figure 6. Effects of 3-bromopyruvic acid (3-BrPA) on glutathione reductase (GR) and glutathione S-transferase (GST) specific activities and the GSH/GSSG ratio. GR and GST activities were measured as U/mg of protein, and the ratio of reduced to oxidised glutathione (GSH/GSSG) was determined following treatment with increasing concentrations of 3-BrPA (μM). Data are presented as mean \pm standard deviation (SD) from 4 independent experiments. A concentration-dependent effect was observed in both enzymatic activities and glutathione redox balance in response to 3-BrPA exposure.

*: $p < 0.05$, **: $p < 0.01$, ***: $p < 0.001$, ****: $p < 0.0001$

Reduced PPP and glycolytic activity lead to increased CPT1C activity upon HK2 inhibition

3-BrPA decreased PPP and glycolytic activity in PDAC cells, addressing reduced energy metabolism, leading to increased CPT1C activation. Upon 3-BrPA administration, CPT1C activation significantly increased in the 1, 20, and 30 μM dose groups compared with the control (Figure 8).

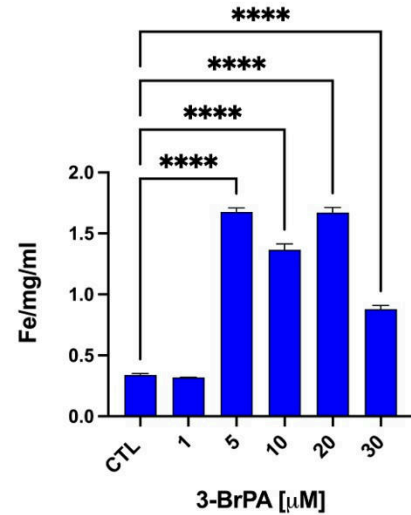


Figure 7. Quantification of the intracellular iron (Fe) content was performed following treatment with 3-bromopyruvic acid (3-BrPA). Total iron levels were measured and expressed as micrograms of iron per milligramme of protein per millilitre ($\mu\text{g Fe/mg/mL}$) after exposure to increasing concentrations of 3-BrPA (μM). Data are reported as the mean \pm standard deviation (SD) from four independent experiments. A concentration-dependent alteration in the intracellular iron content was observed in response to 3-BrPA treatment.

: $p < 0.001$, *: $p < 0.0001$

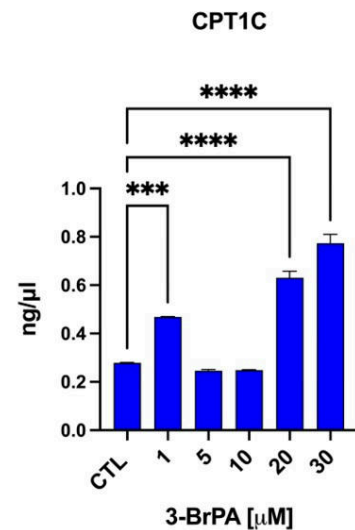


Figure 8. Carnitine palmitoyltransferase 1C (CPT1C) protein levels were quantified following treatment with 3-bromopyruvic acid (3-BrPA). CPT1C concentrations were measured and expressed as ng/ μL after exposure to increasing concentrations of 3-BrPA (μM). Data are reported as the mean \pm standard deviation (SD) from four independent experiments. A concentration-dependent alteration in the CPT1C protein levels was observed in response to 3-BrPA treatment.

: $p < 0.001$, *: $p < 0.0001$

DISCUSSION

Mutations in p53, CDKN2A, and SMAD4 are the most common mutations in PDAC, contributing to metabolic

reprogramming and resistance associated with antioxidant production and inhibiting ferroptosis linked to metastasis and chemoresistance (13). In this study, we investigated 3-BrPA on BXP-3 PDAC cells harbouring p53, CDKN2A, and SMAD4 mutations for the first time in the literature, since inhibiting HK2 may disrupt metabolic pathways critical for cancer survival and trigger ferroptosis, offering a novel therapeutic approach for PDAC theoretically (17). BXP-3 cells were administered increasing concentrations of 3-BrPA for 48 h, and cell viability was evaluated using the MTT assay. IC₅₀ of 3-BrPA was determined to be 40 μ M and (Figure 1) based on the IC₅₀ value, we have determined dosages of the HK2 inhibitor (0, 1, 5, 10, 20, and 30 μ M) for assessing the impact of the 3-BrPA on the ferroptosis, oxidative stress, and metabolic regulation of PDAC cells. To date, no published studies have investigated the anti-cancer effects of 3-BrPA on PDAC cells harbouring concurrent mutations in *TP53*, *SMAD4*, and *CDKN2A*.

In addition to the MTT assay, cell viability and morphological changes indicative of cell death were evaluated via light microscopy following a 48-h incubation with 3-BrPA. Treatment with the HK2 inhibitor significantly reduced cell viability at all tested concentrations relative to the untreated control group, as corroborated by light microscopy observations (Figure 2, Figure 3). Furthermore, HK2 protein levels were quantified in cell lysates from 3-BrPA-treated PDAC cells to determine the inhibitory efficacy of 3-BrPA. A marked reduction in HK2 expression was observed across all treatment concentrations compared with the control group (Figure 4). Collectively, these findings demonstrate that 3-BrPA effectively diminishes PDAC cell viability through the inhibition of HK2 activity.

Subsequent investigations were undertaken to further elucidate the underlying mechanisms driving the compound's anticancer effects. Metabolic reprogramming is a defining hallmark of PDAC, characterised by dysregulation of multiple metabolic pathways, including glucose metabolism, PPP, oxidative phosphorylation (OXPHOS), glutamine metabolism, hypoxia response, and oxidative stress signaling. These alterations play a critical role in promoting chemoresistance, metastasis, and tumour progression across a variety of malignancies, including PDAC (18). This is mainly due to the excessive synthesis and utilisation of substrates essential for bioenergetics and anabolic processes that drive tumour growth, such as glutamine, glucose, lactate, pyruvate, acetate, free fatty acids, and β -hydroxybutyrate, mediated by the upregulation of glycolysis, PPP, and oxidative stress-related metabolic pathways (19). G6PD and 6-PGD are key enzymes in PPP and glycolysis, responsible for generating NADPH. NADPH plays a critical role in maintaining cellular redox

homeostasis by supporting antioxidant enzyme activities, thereby modulating the cellular response to oxidative stress. G6PD and 6-PGD activities significantly decreased in all 3-BrPA-administered groups compared with the control. However, this decrease was significant in the 5, 20, and 30 μ M dose groups (Figure 5), addressing the reduced PPP and glycolysis activity (20).

Ferroptosis, one of the regulated cell death pathways characterised by oxidative stress and iron-dependent lipid peroxidation, has emerged as a significant mechanism underlying chemoresistance and metastasis in PDAC. On the other hand, many therapies aim to induce ferroptosis by using the Fenton reaction, in which Fe^{2+} reacts with H_2O_2 to produce hydroxyl radicals ($\cdot\text{OH}$), initiating lipid peroxidation and oxidative stress. The Fenton reaction involves the catalytic conversion of H_2O_2 into highly reactive hydroxyl radicals ($\cdot\text{OH}$) by ferrous iron (Fe^{2+}). On the other hand, metabolic adaptations such as enhanced glycolysis and activation of the PPP inhibit ferroptosis by sustaining antioxidant defences (21). Given the pancreas's iron-rich microenvironment, the induction of ferroptosis has been proposed as a promising therapeutic strategy for PDAC (10).

In this context, we investigated the activities of GR and GST, along with the levels of reduced and oxidised glutathione (GSH and GSSG, respectively), in PDAC cells to assess cellular oxidative stress and ferroptosis status. GR and GST are key glutathione-dependent antioxidant enzymes that regulate the intracellular redox environment by maintaining the GSH/GSSG ratio, a critical indicator of oxidative stress. GR catalyses the NADPH-dependent reduction of GSSG to regenerate GSH, thereby sustaining the cellular antioxidant defence system and enabling detoxification of reactive oxygen species (ROS). Conversely, GST facilitates the conjugation of GSH to a broad range of electrophilic compounds, including lipid peroxidation products and xenobiotics such as chemotherapeutic drugs, thus enhancing their solubility and promoting their excretion. Disruption in the activities of GR and GST or in the GSH/GSSG balance can compromise redox homeostasis, increase oxidative stress, and sensitise cells to ferroptosis (22). Although recent studies have suggested a correlation between ferroptosis activation and PDAC prognosis, the mechanistic role of ferroptosis in PDAC remains incompletely characterised (23). GR levels decreased in all 3-BrPA-treated groups compared with the control. However, this decrease was only significant for the 20 and 30 μ M dose groups. On the other hand, GST levels significantly increased in the same dose groups compared with the control (Figure 6). The GSH/GSSG ratio decreased across all the treatment groups compared with the control. However, this decrease was

significant in the 5, 20, and 30 μM dose groups (Figure 6). Notably, intracellular Fe levels were significantly elevated in all treatment groups, except at the 1 μM concentration, compared with the control. This increase suggests enhanced oxidative stress and induction of ferroptosis, as further supported by changes in GR, GST, and the GSH/GSSG ratio (Figures 6 and 7), since the importance of the sources of iron within tumours and its biological significance in cancer is associated with ferroptosis (24).

CPT1C belongs to the CPT1 enzyme family involved in the acylation of fatty acids and their subsequent transport into mitochondria for β -oxidation. Cancer cells typically exhibit elevated levels of fatty acid oxidation (FAO), a metabolic adaptation that supports their high energy demands and rapid proliferation (25). CPT1C promotes tumour cell survival under hypoxic and nutrient deprivation conditions and has been identified as a prognostic marker in various human cancers (26). 3-BrPA reduced both PPP and glycolytic activity in PDAC cells, suppressing cellular energy metabolism and upregulating CPT1C activity. Following 3-BrPA treatment, CPT1C activation was significantly increased in the 1, 20, and 30 μM dose groups compared with the control (Figure 8). Our data showed decreased PPP and glycolysis as well as increased CPT1C, which is associated with enhanced FAO and rapid proliferation in PDAC cells. For the first time in the literature, our data showed that 3-BrPA induces ferroptosis and metabolic regulation in PDAC cells via the regulation of PPP, oxidative stress, and glycolysis. Future directions include the *in vivo* validation of 3-BrPA in PDAC models to evaluate its efficacy, pharmacokinetics, and safety. Combining 3-BrPA with standard chemotherapy regimens may overcome resistance

and improve outcomes. Investigating CPT1C-related metabolic adaptations could reveal targetable compensatory pathways, while patient-derived models may identify predictive biomarkers to support personalised treatment strategies.

CONCLUSION

This study provides the first comprehensive analysis of the anticancer effects of 3-BrPA on PDAC cells harbouring concurrent mutations in *TP53*, *SMAD4*, and *CDKN2A*. Our findings demonstrate that 3-BrPA exerts potent cytotoxic effects on BXP-3 cells by targeting HK2, a key regulator of glycolysis and the PPP. Inhibition of HK2 by 3-BrPA significantly reduced G6PD and 6-PGD enzymatic activities, leading to a suppressed glycolytic and PPP flux, diminished antioxidant capacity, and heightened oxidative stress. These metabolic disruptions culminated in elevated intracellular iron levels and a reduced GSH/GSSG ratio, consistent with the induction of ferroptosis. Moreover, the upregulation of CPT1C activity in response to 3-BrPA suggests a metabolic shift towards enhanced fatty acid oxidation, possibly as a compensatory mechanism in response to impaired glucose metabolism. Taken together, these findings indicate that 3-BrPA not only impairs energy production and redox balance in PDAC cells but also promotes ferroptotic cell death, highlighting its potential as a novel therapeutic agent for treating aggressive pancreatic cancers characterised by metabolic reprogramming and resistance to conventional chemotherapy. These *in vitro* findings can guide future *in vivo* studies to explore combinatorial strategies incorporating 3-BrPA with existing chemotherapeutic regimens to overcome treatment resistance and improve clinical outcomes in PDAC.



Acknowledgements The authors gratefully acknowledge the use of the services and facilities of the Koç University Research Centre for Translational Medicine (KUTTAM).

Peer Review Externally peer-reviewed.

Author Contributions Conception/Design of Study- D.A., N.N.U.; Data Acquisition- D.A.; Data Analysis/Interpretation – D.A.; Drafting Manuscript- D.A.; Critical Revision of Manuscript- D.A.; Final Approval and Accountability- D.A.; Technical or Material Support- D.A., N.N.U.; Supervision- D.A.

Conflict of Interest Authors declared no conflict of interest.

Financial Disclosure Authors declared no financial support.

Author Details

Duygu Aydemir

¹ İstanbul University, Institute of Child Health, Department of Pediatric Basic Sciences, Division of Medical Genetics, İstanbul, Türkiye

² Koç University, School of Medicine, Department of Medical Biochemistry, İstanbul, Türkiye

³ Koç University Research Center for Translational Medicine (KUTTAM), İstanbul, Türkiye

ORCID: 0000-0002-6449-2708

Email: duygu.aydemir@istanbul.edu.tr

Nuriye Nuray Uluşu

² Koç University, School of Medicine, Department of Medical Biochemistry, İstanbul, Türkiye

³ Koç University Research Center for Translational Medicine (KUTTAM), İstanbul, Türkiye

ORCID: 0000-0002-3173-1389



REFERENCES

- 1 Sun Y, Ren D, Zhou Y, Shen J, Wu H, Jin X. Histone acetyltransferase 1 promotes gemcitabine resistance by regulating the PVT1/EZH2 complex in pancreatic cancer. *Cell Death Dis* 2021;12(10):878.
- 2 Khaira R, Sharma J, Saini V. Development and characterization of nanoparticles for the delivery of gemcitabine hydrochloride. *ScientificWorldJournal* 2014;2014:560962.
- 3 Ju HQ, Gocho T, Aguilar M, Wu M, Zhuang ZN, Fu J, et al. Mechanisms of overcoming intrinsic resistance to gemcitabine in pancreatic ductal adenocarcinoma through the redox modulation. *Mol Cancer Ther* 2015;14(3):788-98.
- 4 Orth M, Metzger P, Gerum S, Mayerle J, Schneider G, Belka C et al. Pancreatic ductal adenocarcinoma: biological hallmarks, current status, and future perspectives of combined modality treatment approaches. *Radiation Oncology* 2019;14(1):141.
- 5 Liu J, Zhang C, Hu W, Feng Z. Tumor suppressor p53 and metabolism. *J Mol Cell Biol* 2019;11(4):284-92.
- 6 Liu P, Wang Y, Li X. Targeting the untargetable KRAS in cancer therapy. *Acta Pharm Sin B* 2019;9(5):871-9.
- 7 Ghanavat M, Shahrouzian M, Deris Zayeri Z, Banihashemi S, Kazemi SM, Saki N. Digging deeper through glucose metabolism and its regulators in cancer and metastasis. *Life Sci* 2021;264:118603.
- 8 Liu M, Liu W, Qin Y, Xu X, Yu X, Zhuo Q, et al. Regulation of metabolic reprogramming by tumor suppressor genes in pancreatic cancer. *Exp Hematol Oncol* 2020;9(1):23.
- 9 Ping H, Jia X, Ke H. A Novel ferroptosis-related lncRNAs signature predicts clinical prognosis and is associated with immune landscape in pancreatic cancer. *Front Genet* 2022;13:786689.
- 10 Yang Y, Zhang ZJ, Wen Y, Xiong L, Huang YP, et al. Novel perspective in pancreatic cancer therapy: Targeting ferroptosis pathway. *World J Gastrointest Oncol* 2021;13(11):1668-79.
- 11 Fan T, Sun G, Sun X, Zhao L, Zhong R, Peng Y. Tumor energy metabolism and potential of 3-bromopyruvate as an inhibitor of aerobic glycolysis: Implications in tumor treatment. *Cancers (Basel)* 2019;11(3):317.
- 12 Akella NM, Ciraku L, Reginato MJ. Fueling the fire: emerging role of the hexosamine biosynthetic pathway in cancer. *BMC Biol* 2019;17(1):52.
- 13 Otahal A, Aydemir D, Tomasich E, Minichsdorfer C. Delineation of cell death mechanisms induced by synergistic effects of statins and erlotinib in non-small cell lung cancer cell (NSCLC) lines. *Sci Rep* 2020;10(1):959.
- 14 Aydemir D, Hashemkhani M, Acar HY, Ulusu NN. In vitro interaction of glutathione S-transferase-pi enzyme with glutathione-coated silver sulfide quantum dots: A novel method for biodetection of glutathione S-transferase enzyme. *Chem Biol Drug Des* 2019;94(6):2094-102.
- 15 Aydemir D, Hashemkhani M, Acar HY, Ulusu NN. Evaluation of the biocompatibility of the GSH-coated Ag2S quantum dots in vitro: a perfect example for the non-toxic optical probes. *Mol Biol Rep* 2020;47(6):4117-29.
- 16 Fan K, Fan Z, Cheng H, Huang Q, Yang C, Jin K, et al. Hexokinase 2 dimerization and interaction with voltage-dependent anion channel promoted resistance to cell apoptosis induced by gemcitabine in pancreatic cancer. *Cancer Med* 2019;8(13):5903-15.
- 17 Aydemir D, Öztürk K, Arslan FB, Çalis S, Ulusu NN. Gemcitabine-loaded chitosan nanoparticles enhanced apoptotic and ferroptotic response of gemcitabine treatment alone in the pancreatic cancer cells in vitro. *Naunyn Schmiedeberg's Arch Pharmacol* 2024;397:9051-66.
- 18 Zheng P, Pan HH, Zhou XH, Qiu YY, Hu J, Qin ZS, et al. Glucose 6 phosphatase dehydrogenase (G6PD): a novel diagnosis marker related to gastrointestinal cancers. *Am J Transl Res* 2023;15(4):2304-28.
- 19 Anapali M, Kaya-Dagistanli F, Akdemir AS, Aydemir D, Ulusu NN, Ulutin T, et al. Combined resveratrol and vitamin D treatment ameliorate inflammation-related liver fibrosis, ER stress, and apoptosis in a high-fructose diet/streptozotocin-induced T2DM model. *Histochem Cell Biol* 2022;158(3):279-96.
- 20 Li L, Yu X, Gao L, Cheng L, Sun B, Wang G. Diabetic ferroptosis and pancreatic cancer: Foe or friend? *Antioxid Redox Signal* 2022;37(16-18):1206-21.
- 21 Aydemir D, Malik AN, Kulac I, Basak AN, Lazoglu I, Ulusu NN. Impact of the amyotrophic lateral sclerosis disease on the biomechanical properties and oxidative stress metabolism of the lung tissue correlated with the human mutant SOD1G93A protein accumulation. *Front Bioeng Biotechnol* 2022;10:810243.
- 22 Cao JY, Dixon SJ. Mechanisms of ferroptosis. *Cell Mol Life Sci* 2016;73(11-12):2195-209.
- 23 Huang Z, Ma Y, Sun Z, Cheng L, Wang G. Ferroptosis: potential targets and emerging roles in pancreatic diseases. *Arch Toxicol* 2024;98(1):75-94.
- 24 Zhou Y, Chen Y, Zhao P, Xian T, Gao Y, Fan S, et al. The YY1-CPT1C signaling axis modulates the proliferation and metabolism of pancreatic tumor cells under hypoxia. *Biochem Pharmacol* 2024;227:116422.
- 25 Fadó R, Zagmutt S, Herrero L, Muley H, Rodríguez-Rodríguez R, Bi H, et al. To be or not to be a fat burner, that is the question for cpt1c in cancer cells. *Cell Death Dis* 2023;14(1):57.

